Research on Chemical Intermediates (2021) 47:2573–2587
https://doi.org/10.1007/s11164-021-04426-6

Catalytic activity of gold nanoparticles deposited on N-doped carbon-based supports in oxidation of glucose and arabinose mixtures

Sebastian Franz[1] · Nataliya D. Shcherban[2] · Igor Bezverkhyy[3] · Sergii A. Sergiienko[4] · Irina L. Simakova[5] · Tapio Salmi[1] · Dmitry Yu. Murzin[1]

Received: 13 November 2020 / Accepted: 27 February 2021 / Published online: 9 March 2021

Abstract

Oxidation of a mixture of glucose and arabinose over Au particles deposited on porous carbons, N-doped carbons and carbon nitrides was investigated at 70 °C, under constant pH of 8, and oxygen partial pressure 0.125 atm. In particular, Au deposited on nitrogen-containing carbon-based mesoporous structures demonstrated activity in the oxidation of the sugars to the corresponding aldonic acids higher than gold deposited on undoped carbon supports (conversion of glucose up to ca. 60%, arabinose–ca. 30% after 200 min). The results can be explained by the basic nature of the supports leading to an increase in the polarity of the carbon surface and the oxygen activation. Glucuronic acid (with selectivity ca. 10–93.5%) together with gluconic acid was formed as a result of glucose oxidation, while arabinose was selectively oxidized to arabinonic acid.

Keywords Sugar oxidation · Gold catalysts · Glucose · Arabinose · Carbon support · Glucuronic acid

✉ Nataliya D. Shcherban
nataliyalisenko@ukr.net

[1] Laboratory of Industrial Chemistry and Reaction Engineering, Johan Gadolin Process Chemistry Centre, Åbo Akademi University, Biskopsgatan 8, 20500 Abo/Turku, Finland

[2] L.V. Pisarzhevsky Institute of Physical Chemistry, National Academy of Sciences of Ukraine, 31 pr. Nauky, Kyiv 03028, Ukraine

[3] Laboratoire Interdisciplinaire Carnot de Bourgogne, UMR 6303 CNRS-Université de Bourgogne-Franche Comté, 9 Av. A. Savary, BP 47870, 21078 Dijon Cedex, France

[4] Department of Materials and Ceramics Engineering, CICECO-Aveiro Institute of Materials, University of Aveiro, 3810-193 Aveiro, Portugal

[5] Boreskov Institute of Catalysis, Lavrentieva ave. 5, Novosibirsk, Russia 630090

Introduction

Gold nanoparticles deposited onto various porous supports afford high activity and selectivity in low-temperature oxidation of CO, carbohydrates and aldehydes [1–6]. They are also characterized by a superior durability, being highly resisted to deactivation. Such deactivation is typically provoked by over-oxidation and corresponding poisoning (by the reaction products, i.e., aldonic acids) of the catalytically active metal phase [7]. Alumina- supported gold nanoparticles were reported to be highly active in the oxidation of sugars under mild conditions (50–70 °C, pH 6–9, atmospheric pressure) [8, 9]. Structure sensitivity in the oxidation reactions implies the key role of the gold nanoparticles size among other factors determining catalytic activity [4, 10]. As an example, Au particles of ca. 2.5 nm exhibit the highest catalytic performance in arabinose oxidation [9].

In terms of sustainable development, an increasing attention is attracted by utilization of natural resources, namely lignocellulosic biomass, for the catalytic processing of corresponding sugars into various value-added products [11, 12]. For instance, hydrolysis of hemicelluloses can be performed over both homogeneous and heterogeneous catalysts [13]. The resulting molecules of sugars can be subjected to further processing including hydrogenation, isomerization or oxidation leading to different valuable chemicals. In the case of oxidation, aldonic acids are the desired products. Being biodegradable and biocompatible [12] they are widely applied in medicine, cosmetics, food and detergent industries [14, 15].

Oxidation of binary glucose and arabinose mixtures over alumina-supported gold nanoparticles was investigated in the previous work [16]. It was shown that under all studied conditions (the temperature range of 50–80 °C, pH 7–9, $pO_2 = 0.0625–0.25$ bar), arabinose oxidation was more favorable. A kinetic model capable of explaining the experimental data on oxidation of arabinose and glucose mixtures at different conditions and also considering aldo-ketose isomerization was developed [16].

Porous carbon materials possessing high specific surface area, large pore volume, chemical inertness, high thermal stability and mechanical strength as well as low production costs have numerous applications in adsorption and catalysis [17]. However, as far as the oxidation of sugars is concerned, it has been shown that the carbon-supported gold nanoparticles exhibit a low catalytic activity in the oxidation of sugars such as glucose [4] and arabinose [18]. It is known [19] that carbon supports have only weak interactions with the catalytically active phase and they adsorb sugars to a certain extent due to a large surface area, which has been used as an explanation of a stronger dependence of the reaction rate on the sugar concentration and the reaction temperature using carbon supports instead of metal oxides [4]. On the contrary, metal oxides as supports might influence gold clusters electronically resulting in a weaker rate dependence than with Au/carbon and unsupported Au colloids [4].

Typically, the application of carbon supports for Au deposition using classical catalyst preparation methods such as deposition–precipitation results in the formation of much larger nanoparticles with a broad distribution than in the case

of oxide supports. For the preparation of smaller carbon-supported Au nanoparticles, special conditions such as the application of organogold complexes [4, 20] or stabilizing agents such as polymers or surfactants [21, 22] are required.

Utilization of nitrogen-containing carbons instead of pure carbons as supports for gold deposition seems to be an effective way to increase the catalytic activity of supported Au particles. It can be hypothesized that N-containing sites present in N-doped carbon supports could strengthen interactions between the metal and the support because of polarization sites.

The aim of the current paper was to investigate the oxidation of model glucose and arabinose mixtures over gold nanoparticles supported on N-doped carbons and carbon nitrides. These sugars were selected as there exists a wealth body of the literature for oxidation of the individual components in this mixture. For the sake of comparison, undoped microporous and mesoporous carbons as well as alumina were used for gold deposition.

Experimental section

Catalysts preparation

The carbon support labeled as C-micro was prepared by bulk pyrolysis of sucrose at 900 °C for 2.5 h.

Graphitic carbon nitride C_3N_4 was obtained by pyrolysis of melamine according to the procedure described in [23]. Melamine (Merck, ≥ 99%) was placed in the middle of a quartz tube and heated under argon flow at 300 °C for 1 h, and then at 600 °C for 2 h.

For preparation of mesoporous carbon supports labeled as C-MCF, C-N-MCF, C-N-MCF-Ox and C_xN_y-MCF mesoporous cellular foam MCF was used as a hard template. C-MCF was synthesized by carbonization of sucrose in the presence of sulfuric acid as a catalyst in silica pores. MCF (1 g) was mixed with an aqueous solution (ca. 5 ml) containing sucrose (Carlo Erba, ≥ 99%, 1.69 g) and concentrated H_2SO_4 (0.19 g). The obtained suspensions were heated at 100 °C for 6 h, and then at 160 °C for the same time. Then, the composite contained partly decomposed sucrose was mixed again with an aqueous solution of sucrose and sulfuric acid (1.08 and 0.12 g, respectively). After the thermal treatment in the identical conditions, the obtained dark-brown powder was heated (heating rate 4 °C/min) in argon to 900 °C and kept at this temperature for 2.5 h.

For the synthesis of C-N-MCF 1.2 g of the obtained carbon–silica composite based on MCF was treated with an ethanol solution of melamine (0.26 g of melamine in 1.3 ml of ethanol) and stirred at room temperature for 5 h. The resulting suspension was boiled to evaporate the alcohol followed by drying at 120 °C. The impregnated sample was heated in argon up to 950 °C (heating rate 10 °C/min) and kept at this temperature for 0.5 h. The obtained sample was then washed with hot distilled water to neutral pH of the wash water in order to remove all residues of melamine decomposition products.

For the preparation of C-N-MCF-Ox the obtained carbon–silica composite based on MCF was preliminarily oxidized with 45% nitric acid (Macrochem) for 4 h, after which the sample was washed with distilled water to remove an excess acid and water-soluble oxidation products and dried at 100 °C. Functionalization of the obtained oxidized product with nitrogen was carried out using melamine as described above for C-N-MCF material.

C_xN_y-MCF was prepared by pyrolysis of ethylenediamine and carbon tetrachloride. For this purpose, 0.5 g MCF was added to the mixture containing 1.8 ml of ethylenediamine (Merck, ≥ 99%) and 2.0 ml of CCl_4 (Macrochem, ≥ 98%) and heated to 90 °C for 6 h under reflux. The resulting dark-brown suspension was dried at 60 °C and then heated at 400 °C for 2 h. The obtained powder was mixed with a mixture of 0.9 ml of ethylenediamine and 1.0 ml of carbon tetrachloride. The mixture was re-heated to 90 °C for 6 h under reflux and dried at 60 °C. The obtained brown powder was heated in an inert atmosphere up to 600 °C (heating rate 3 °C/min) and kept at this temperature for 5 h.

For all the above silica-containing composites, the silica template was removed by treatment in HF (Merck, 40%) solution (HF: $H_2O = 1$: 3). The obtained products were washed with distilled water and ethanol several times and then dried at 100 °C overnight.

For the preparation of Au-supported catalysts (2 wt.% of Au), the corresponding supports were precalcined at 150 °C for 2 h and then loaded with gold obtained from hydrogen tetrachloroaurate $HAuCl_4$ (Acros Organics, 99.999%) using the following procedure adapted from [24, 25]. First 1 g of the support was added to 25 mL of 4.2×10^{-3} M $HAuCl_4$ aqueous solution containing urea (0.42 M). The mixture was heated under vigorous stirring (250 rpm) at 90 °C for 24 h, after which the mixture was cooled, centrifuged, washed, dried overnight at 60 °C and calcined in air at 250 °C (10 °C/min) for 2 h.

For comparison, alumina-supported Au catalyst (Au/Al_2O_3) previously shown as a highly active material in sugar oxidation was synthesized via the deposition–precipitation method described in [26]. A 1.6×10^{-3} M aqueous solution of $HAuCl_4$ with urea (0.21 M) was mixed with Al_2O_3 as a powder followed by heating at 81 °C for 4 h. After filtration, the catalyst was washed with distilled water and then additionally with a 25 M NH_4OH solution to remove the excess chloride after deposition of gold. Thereafter, the catalyst was washed with water, filtered and dried at room temperature for 24 h. This was followed by calcination in air at 350 °C (2 °C/min).

Characterization

The phase composition of the samples was analyzed using X-ray diffractometer D8 ADVANCE (Bruker AXS) with CuK_α-radiation.

Nitrogen ad(de)sorption was measured by a volumetric method (77 K, up to 1 atm) using Sorptomatic 1990 (Thermo Electron Corp). The samples were evacuated ($P \leq 0.7$ Pa) at 300 °C for 4 h prior to the measurements. The specific surface area (S_{BET}) was calculated by the BET equation [27], and the mesopore sizes were evaluated from the desorption branches of the isotherm, using the method

of Barrett–Joyner–Halenda (BJH) [28]. The comparative *t*-plot method [29] was applied to determine the micropore and mesopore volumes as well as the mesopore surface area.

SEM (scanning electron microscopy) images were obtained using the field emission SEM FEI Quanta 200 FEG. Images were generated using an accelerating voltage of 15–20 kV and a beam current of 0.65 nA. Before imaging the samples were coated, using a sputtering method, by platinum film of 15 nm thickness.

TEM (transmission electron microscopy) images were obtained using the field emission TEM JEM-2100F (JEOL) with an accelerating voltage of 200 kV. A sample was dispersed in ethanol in an ultrasonic bath for 5 min followed by the suspension deposition to a copper grid coated with a carbon film.

XPS (X-ray photoelectron spectroscopy) analysis of the supports was performed using PerkinElmer PHI 5400 spectrometer with a Mg K_α X-ray source operated at 14 kV and 200 W. The samples were kept in the introduction chamber of the XPS equipment overnight before the analysis. The pass energy of the analyzer was 17.9 eV and the energy step 0.1 eV. The charging was adjusted according to the C–C bond at 284.5 eV. Peak fitting was performed with the program XPS Peak 4.1. The background was corrected with the Shirley function. The sensitivity factors used in the quantitative analysis for C 1 s and N 1 s were 0.296 and 0.477, respectively.

Catalytic tests

The experiments for oxidation of glucose and arabinose mixtures were performed in a laboratory-scale glass reactor equipped with an efficient mechanical stirrer and a heating jacket (the scheme of the reactor setup is presented in Fig. A.) The reaction was conducted in a semi-batch mode under a constant gas flow of O_2 in Ar. A Brooks 5850S device was used in order to control and adjust the gas feed. Temperature and pH were controlled using a Metrohm Titrando 907 device equipped with a Metrohm Unitrode electrode.

The reactor was flushed with argon (c.a. 65 ml/min) and heated to the desired reaction temperature. During flushing, the dry catalyst with a particle size smaller than 65 μm (for the suppressing the internal mass transfer limitations in the catalyst pores) was added into the reactor. At the same time, a solution of L-arabinose (Sigma-Aldrich, $\geq 99\%$) and anhydrous D-glucose (Fluka, $\geq 98\%$) with the mass ratio of 1:1 was heated to c.a. 40–50 °C under vigorous stirring to minimize the temperature difference at the beginning of the reaction. The total volume of the solution having the concentration 2 g in 100 ml was 150 ml. After a complete flushing of the reactor vessel, the sugar solution was added into the reactor and heated in argon atmosphere to the desired reaction temperature under stirring (1000 rpm) and pH control (pH 8). Upon reaching the reaction temperature, the argon flow was decreased to the desired value and the pre-adjusted oxygen was introduced into the argon flow, resulting in a total gas flow of 40 ml/min. The pH control was carried out using 1 M NaOH.

The samples were periodically withdrawn from the liquid phase during the experiments and the concentration profiles of the reactants, and the reaction products were

monitored using high-performance liquid chromatography (VWR Hitachi Chromaster) equipped with a 300×7.8 mm Bio-Rad Aminex HPX-87C column and a RI detector (VWR Hitachi Chromaster 5450). The operating temperature of the column was 80 °C and the flow rate of 0.6 ml/min using 1.2 mM $CaSO_4$ as an eluent, operating in the isocratic mode, and resulting in a column backpressure ranging between 65 and 70 bar. The injection volume of the investigated sample was 10 µl.

Results and discussion

Catalyst characterization

Characterization of the phase composition of the prepared supports was performed using X-ray diffraction (XRD) (Fig. 1). Carbons and N-doped carbons possess an amorphous structure due to the so-called turbostratic structure, which is characterized by different graphite layers stacking ordering degree. The diffraction pattern of C_xN_y-MCF contains a broad reflex at $2\theta = 25.4°$ (Fig. 1a) corresponding to the diffraction from the plane (002) with the interplanar distance of 0.351 nm, which is close to the interplanar distance in carbon nitride of such a composition. XRD pattern of graphitic carbon nitride C_3N_4 possesses one major reflex (002) at $2\theta \sim 27.3°$ (Fig. 1a) corresponding to an average interplanar distance of 0.327 nm which is typical for interplanar distances in ordered layers of conjugated aromatic systems.

The samples prepared using silica MCF as a hard template are characterized by a high degree of spatial ordering (Fig. 1b). Peak position and intensity of low-angle reflexes for N-doped carbons and C_xN_y-MCF are similar to those ones in mesoporous carbon without nitrogen. Incorporation of nitrogen leads to a slight shift of the low-angle reflexes in the diffraction pattern which can be associated with a corresponding minor change of interatomic distances and electron-donor properties

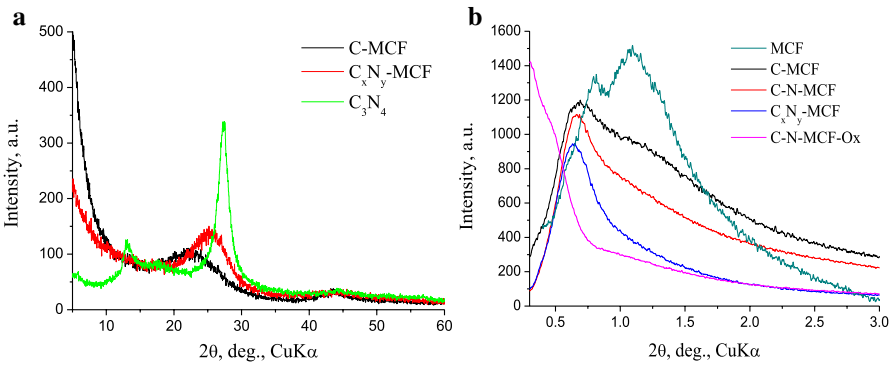

Fig. 1 XRD patterns of the initial supports in middle-angle (**a**) and small-angle (**b**) regions

of nitrogen. The disordered mesostructure of C-N-MCF-Ox is evidently caused by an oxidative treatment of the corresponding carbon–silica composite.

The applied MCF-based supports are characterized by a predominantly mesoporous structure (V_{meso} up to 0.73 cm^3/g, $V_{micro} = 0.01–0.08$ cm^3/g), comparatively high specific surface area (S_{BET}—up to 530 m^2/g), total pore volume (V_{Σ}—up to 0.81 cm^3/g), but low mesopore size uniformity due to the difficulties of the replication process of the porous structure of the initial silica matrix MCF (Table 1).

An increase in the nitrogen content in the products of the initial matrices replication leads to a decrease in the total adsorption volume of the prepared samples. It can be associated with the complex formation of a monolithic rigid framework in the mesopores of silica hard template especially in the case of carbon nitride with a dense framework. Carbon sample C-micro is characterized by a microporous structure with the micropore volume of 0.26 cm^3/g. The total pore volume includes ca. 90% of micropores ($D_{micro} \leq 1$ nm) indicating a high uniformity of microporous structure in the prepared material (Table 1). Graphitic carbon nitride C_3N_4 contains large mesopores (D_{meso} ca. 50 nm) resulting in low total pore volume.

As can be seen from the SEM images (Fig. 2), all Au-supported samples contain large gold particles (particle size is within the range of ca. 10–150 nm). Moreover, the particle distribution is not uniform. Only the catalyst denoted as Au/C-micro possesses much smaller gold particles (ca. 10–20 nm) distributed more homogeneously than in the other ones.

According to the TEM measurements, carbon-supported Au catalysts contain gold particles with diameters ranging from 10 to 45 nm (Fig. 3), the maxima in the particle size distributions correspond to 20–30 nm. On the contrary, Au/Al_2O_3 typically possesses predominantly small gold nanoparticles (Fig. B) with an average particle size of 2.2 nm.

Catalytic activity and selectivity

Selective oxidation of the glucose and arabinose mixture to the corresponding aldonic acids (Fig. 4) was carried out isothermally at atmospheric pressure, in

Table 1 Parameters of the porous structure of the supports (N_2, 77 K)

Support	V_{micro}, cm^3/g	V_{meso}, cm^3/g	D_{meso}, nm	S_{meso}, m^2/g	S_{BET}, m^2/g	V_{Σ}, cm^3/g
C-MCF	0.01	0.73	4.0	420	450	0.74
C_xN_y-MCF	0.08	0.54	4.1 ± 1.5 18.4 ± 4.0 48.5 ± 4.3	330	530	0.81
C-micro	0.26	0.01	> 3	2	745	0.29
C_3N_4	0.00	0.06	~50	10	10	0.06

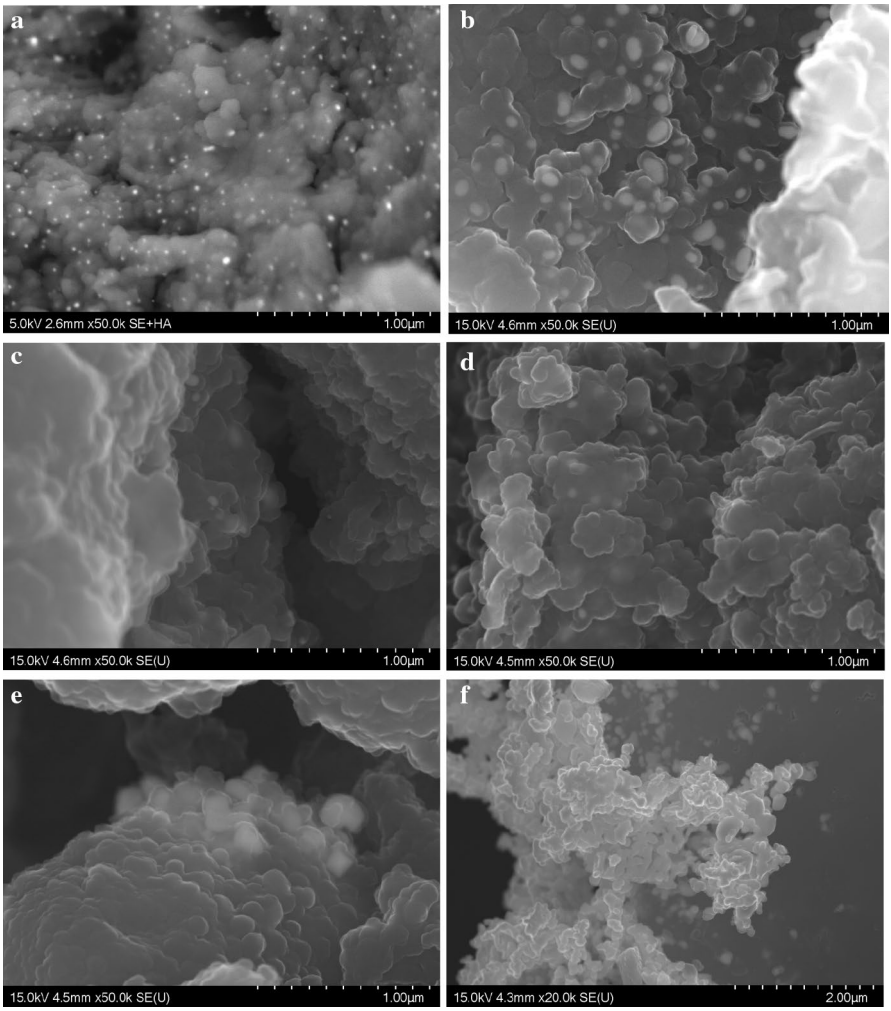

Fig. 2 SEM images of the supported gold samples: **a**—Au/C-micro, **b**—Au/C-MCF, **c**—Au/C-N-MCF, **d**—Au/C-N-MCF-Ox, **e**—Au/C_xN_y-MCF, **f**—Au/C_3N_4

aqueous phase in semi-batch mode. The reactant was introduced in a batch mode, and the oxidant was fed continuously. The catalytic data were obtained in the kinetic regime which was confirmed by evaluation of the liquid-to-solid mass transport limitations and intraparticle diffusion limitations similar to [18].

Typical concentration curves of the sugars mixture oxidation over Au catalysts deposited onto different carbon-based supports, plotted against the normalized

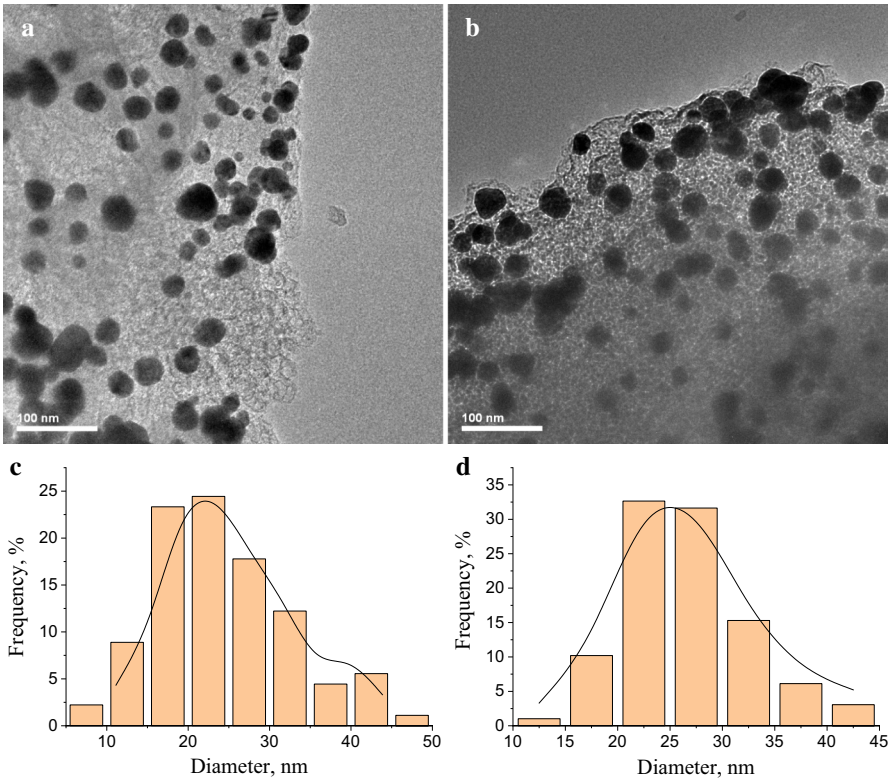

Fig. 3 TEM-images and corresponding particle size distributions for the supported gold catalysts: **a**, **c**—Au/C-MCF, **b**, **d**—Au/C-N-MCF

time (i.e., time multiplied by the amount of gold to compensate for small variations in the exact amounts of catalyst in different experiments) are presented in Fig. 5, which reveals that glucose and arabinose were oxidized to the corresponding aldonic acids, namely gluconic, glucuronic and arabinonic acids.

The effect of the mass ratio of glucose to arabinose on the catalytic activity and selectivity for one gold catalyst (namely Au/Al_2O_3) has been investigated in the previous contribution of the paper [16]. In particular, the mixtures with different sugar molar ratios (arabinose/glucose = 1:0, 0.75:0.25, 0.5:0.5, 0.25:0.75, 0:1) as well as individual sugars have been studied. In general, rather similar oxidation rates for sugars when they were used as individual compounds or in mixtures, were obtained, even if oxidation of arabinose was slightly preferred.

The obtained catalytic data on the glucose and arabinose mixture oxidation over different Au-supported catalysts are provided in Table 2 showing the initial

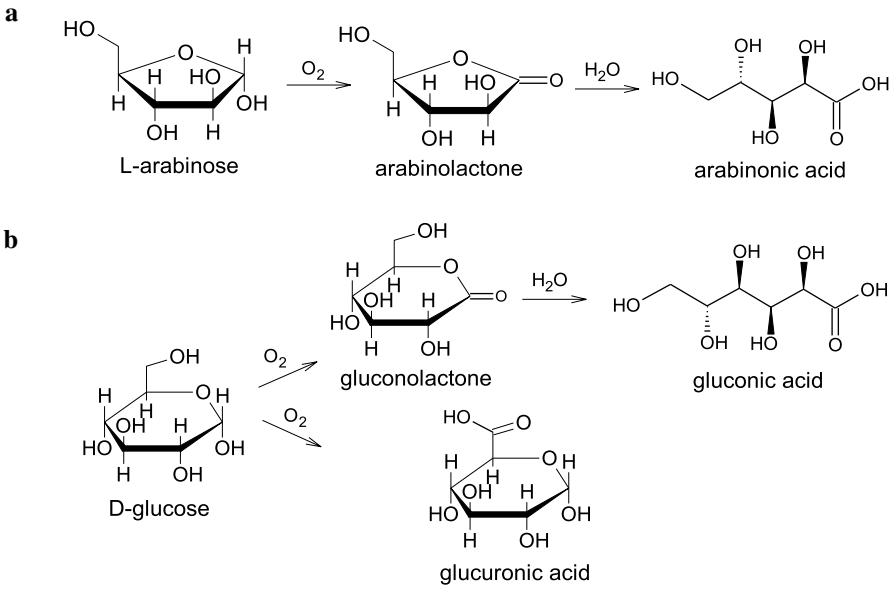

Fig. 4 Reaction scheme for selective oxidation of arabinose (**a**) and glucose (**b**) over supported gold catalysts

reaction rates, sugar conversions and selectivities to the main products, i.e., the aldonic acids.

As can be seen from Table 2, the sugar conversion was rather low over all studied carbon-based Au catalysts, while the alumina-supported Au catalyst showed a high reaction rate and almost complete conversion. The initial reaction rates were low for Au deposited on the prepared carbon-based supports, whereas according to the previous studies [18], Au on metal oxides allowed higher initial oxidation rates. A low initial reaction rate obtained with the carbon support in ref. [18] was due to a broad particle size distribution of Au particles in Au/C being in the range from 3 to 80 nm. On the contrary, gold nanoparticles deposited on metal oxides had a uniform and narrow distribution between 2.3 and 2.8 nm [18]. The preferred glucose oxidation in its mixture with arabinose over carbon-based supported materials can be associated with the preferential glucose adsorption on N-doped supports. This difference between glucose and arabinose oxidation in their mixture is not visible of alumina-supported gold nanoparticles (Fig. 5g). The selectivity toward the main products was high, in particular, arabinonic acid was the only reaction product in arabinose oxidation, whereas glucose oxidation over carbon-based supported catalysts led to the formation of gluconic and glucuronic acids (Fig. 4, Table 2). At the same time, glucuronic acid was not formed

over Au/Al_2O_3, which might indicate the role of the support in the formation of glucuronic acid. It should be emphasized that typically glucose is oxidized only to gluconic acid over gold nanoparticles [4, 20]. In the present work, glucose oxidation resulted both in gluconic and glucuronic acids with a selectivity toward the latter one within the range of 10–93% (Table 2). The data in the literature concerning catalytic oxidation of glucose to glucuronic acid are scarce. For instance, direct oxidation of D-glucose to glucuronic acid (53% yield) over cesium-promoted gold nanoparticles has been reported [30]. Glucuronic acid is a very valuable chemical and it can be applied in pharmaceutical and alimentary industries being an intermediate for the production of hyaluronic acid [31].

In comparison with the gold particles deposited on carbon which were described in ref. [32] where Au particles size ranged from 3 to 80 nm, the particles with sizes less than 10 nm are absent in the most active catalyst (Au/C-N-MCF, Fig. 3d) investigated in the current work. According to [20] such large gold particles are supposed to be inactive in sugar oxidation. However, some of the prepared catalysts exhibited catalytic activity despite a large gold cluster size. It should be pointed out that Au deposited onto N-doped carbon supports (Au/C-N-MCF and Au/C_xN_y-MCF) was catalytically active. It can be associated with the basic nature of the applied supports and a subsequent increase in the carbon surface polarity. Formed polar N-containing groups probably can increase the adsorption and activation of oxygen thus enhancing the reactivity of the supported catalyst.

The nature of basicity of the applied N-containing carbons was investigated with XPS. XPS spectra of the N-doped supports C-N-MCF and C_xN_y-MCF in active catalysts are presented in Fig. 6. The deconvolution of the N 1 s region of the XPS spectrum of the nitrogen-containing sample C-N-MCF gives four peaks (Fig. 6a) corresponding to pyridinic N (398.7 eV), pyrrolic N (400.1 eV), quaternary N (401.1 eV) and pyridine-N-oxide (402.2 eV) [32]. The highest amounts of nitrogen are presented by pyridinic and pyrrolic N (ca. 35 at% for each type).

N 1 s region of the XPS spectrum of carbon nitride CxNy-MCF can be deconvoluted into two peaks (Fig. 6b) attributed to nitrogen bonded to the sp^2 carbon in the aromatic ring (398.5 eV) and nitrogen trigonally bonded to all sp^2 carbons (400.8 eV) [33].

According to the literature [34, 35], nitrogen incorporated into the carbon structure (ca. carbon nanotubes) promotes the activation of oxygen due to formation of the additional electronic states around the Fermi level. The donated electrons can migrate to adsorbed oxygen molecules enhancing their reactivity in particular in ethanol oxidation [35]. The supports applied in the current work possess corresponding nitrogen species (graphite- and pyridine-like nitrogen, Fig. 6) which can activate oxygen resulting in elevated activity of the prepared Au-supported catalysts in sugars oxidation, compared to N-free materials.

The obtained results seem to be promising for further development of carbon-supported gold catalysts in particular for glucose oxidation to glucuronic acid.

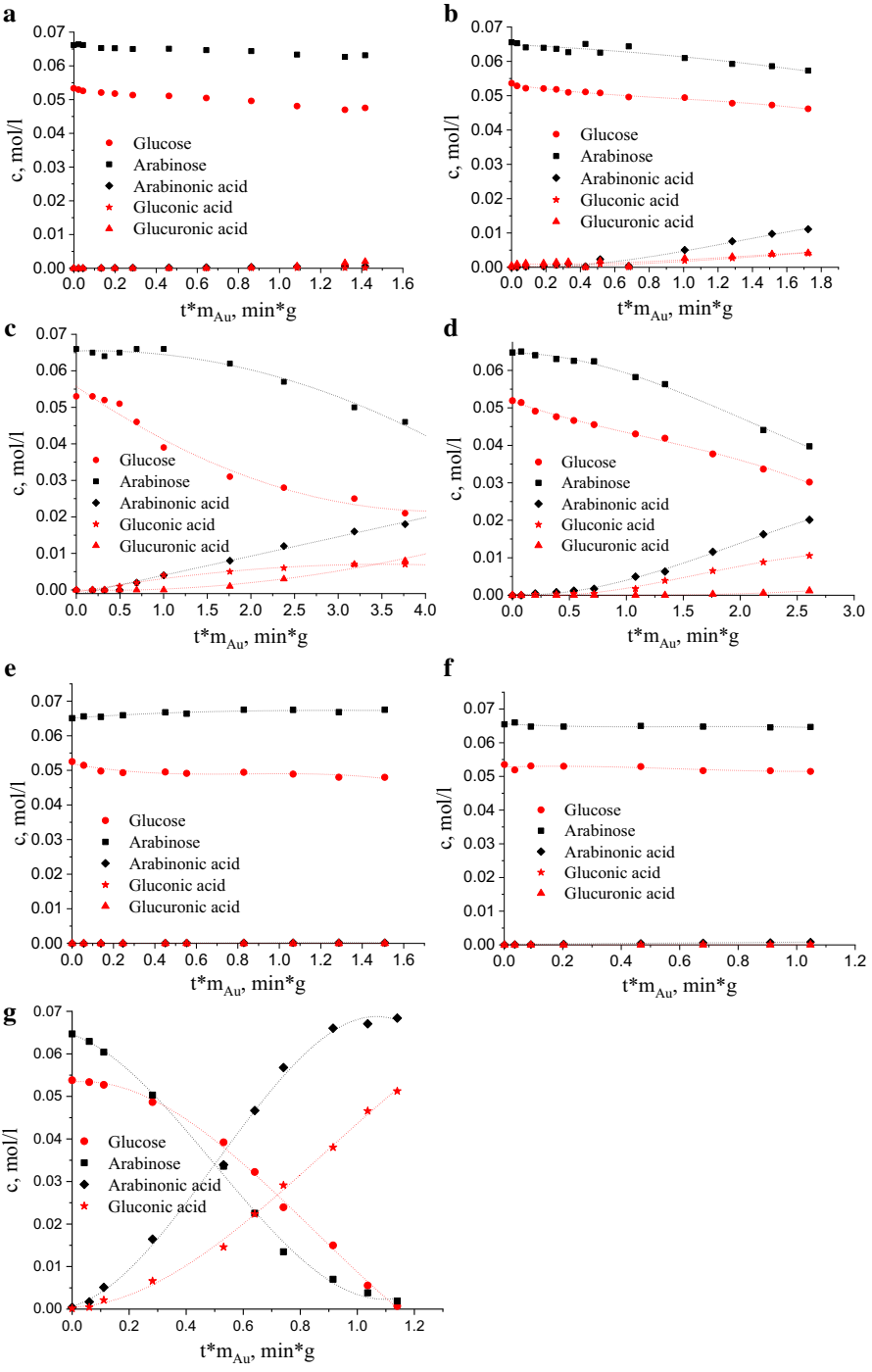
a
b
c
d
e
f
g
c, mol/l
t*m$_{Au}$, min*g
Glucose
Arabinose
Arabinonic acid
Gluconic acid
Glucuronic acid

◀ **Fig. 5** Kinetic curves for oxidation of the glucose and arabinose mixture over supported gold catalysts: **a**—Au/C-micro, **b**—Au/C-MCF, **c**—Au/C-N-MCF, **d**—Au/C_xN_y-MCF, **e**—Au/C_3N_4, **f**—Au/C-N-MCF-Ox, **g**—Au/Al_2O_3. Conditions: 70 °C, pH 8, $pO_2 = 0.125$ atm

Table 2 Comparison of the catalytic behavior in glucose and arabinose mixture oxidation (70 °C, pH 8, $pO_2 = 0.125$ atm)

Catalyst	Initial oxidation rate $*10^{-3}$ (mol/$g_{metal} \times$min)	Conversion after 200 min (%)			Selectivity toward aldonic acids after 200 min (%)		
	Glucose	Arabinose	Glucose	Arabinose	Gluconic acid	Glucuronic acid	Arabinonic acid
Au/C-micro	1.1	0.6	10.9	4.6	6.5	93.5	100
Au/C-MCF	0.7	0.8	13.9	7.1	49.3	50.7	100
Au/C-N-MCF	7.0	1.4	59.9	29.8	48.0	52.0	100
Au/C_xN_y-MCF	1.2	0.8	41.9	10.2	89.8	10.2	100
Au/C_3N_4	0.8	0.3	8.7	3.8	100	0	100
Au/C-N-MCF-Ox	0.2	0.1	3.8	1.2	100	0	100
Au/Al_2O_3	37	69	98.0	96.0	100	0	100

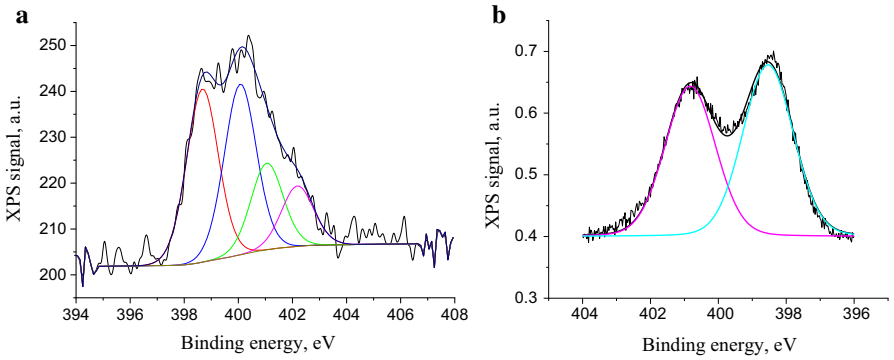

Fig. 6 XPS spectra of **a** C-N-MCF and **b** C_xN_y-MCF

Conclusions

Oxidation of a mixture of glucose and arabinose over gold particles supported on porous carbon materials, N-doped carbons and carbon nitrides was studied. Despite a large Au cluster size (the maxima in the particle size distributions 20–30 nm), Au

deposited on nitrogen-containing carbon mesoporous structures in contrast to gold deposited on undoped carbon supports was found to be active in the oxidation of glucose and arabinose to aldonic acids. The basic nature of these supports results in an increase in the polarity of the carbon surface thus enhancing the activation of oxygen. Preferred glucose oxidation in the investigated mixture was observed. Arabinose was oxidized into arabinonic acid, whereas glucose oxidation resulted in the formation of gluconic and glucuronic acids.

Supplementary Information The online version contains supplementary material available at (https://doi.org/10.1007/s11164-021-04426-6).

Acknowledgements Financial support from Åbo Akademi University (Chancellor's Gadd Prize, D. Yu. Murzin) and Academy of Finland (Academy Professor's grant 319002, T. Salmi) is gratefully acknowledged. The authors are grateful to A. Aho for XPS measurements. NS acknowledges the support of the National Academy of Sciences of Ukraine to the project "New effective nanoscale catalysts for the production of valuable organic compounds from bio raw materials and products of its conversion" (0120U100182). IS acknowledges the financial support of the Ministry of Science and Higher Education of the Russian Federation within the governmental order for Boreskov Institute of Catalysis (Project AAAA-A21-121011390055-8).

Funding Open access funding provided by Abo Akademi University (ABO).

Data availability The present research results have not been published before. Data and Materials are all in the main text, figures and tables.

Declarations

Conflict of interests The authors declare that they have no competing interests.

References

1. M. Haruta, Chem. Rec. **3**, 75 (2003)
2. N. Lopez, T.V.J. Janssens, B.S. Clausen, Y. Xu, M. Mavrikakis, T. Bligaard, J.K. Nørskov, J. Catal. **223**, 232 (2004)
3. S. Chayaporn, C. Thunyaratchatanon, A. Luengnaruemitchai, Res. Chem. Intermed. **46**, 4173 (2020)
4. T. Ishida, N. Kinoshita, H. Okatsu, T. Akita, T. Takei, M. Haruta, Angew. Chem. Int. Ed. **120**, 9405 (2008)
5. A. Corma, M.E. Domine, Chem. Commun. **32**, 4042 (2005)
6. A.S.K. Hashmi, K. Stephen, Chem. Rev. **107**, 3180 (2007)
7. A. Mirescu, U. Prüße, Appl. Catal. B Environ. **70**, 644 (2007)
8. B.T. Kusema, DYu. Murzin, Catal. Sci. Technol. **3**, 297 (2013)

9. B.T. Kusema, B.C. Campo, O.A. Simakova, A.R. Leino, K. Kordas, P. Mäki-Arvela, T. Salmi, DYu. Murzin, ChemCatChem **3**, 1789 (2011)
10. M. Haruta, Catal. Today **36**, 153 (1997)
11. J.N. Chheda, G.W. Huber, J.A. Dumesic, Angew. Chem. Int. Ed. **46**, 7164 (2007)
12. C. Baatz, U. Prüße, Catal. Today **122**, 325 (2007)
13. B.T. Kusema, C. Xu, P. Mäki-Arvela, S. Willför, B. Holmbom, T. Salmi, D.Yu. Murzin, Int. J. Chem. Reactor Eng. **8**, 1 (2010)
14. T. Ishida, H. Watanabe, T. Bebeko, T. Akita, M. Haruta, Appl. Catal. A Gen. **377**, 42 (2010)
15. A.V. Tokarev, E.V. Murzina, K. Eränen, H. Markus, A.J. Plomp, J.H. Bitter, P. Mäki-Arvela, D.Y. Murzin, Res. Chem. Intermed. **35**, 155 (2009)
16. S. Franz, N.D. Shcherban, I.L. Simakova, M. Peurla, K. Eränen, J. Wärnå, T. Salmi, DYu. Murzin, React. Kinet. Mech. Cat. **132**, 59 (2021)
17. B. Sakintuna, Y. Yürüm, Ind. Eng. Chem. Res. **44**, 2893 (2005)
18. B.T. Kusema, B.C. Campo, P. Mäki-Arvela, T. Salmi, DYu. Murzin, Appl. Catal. A Gen. **386**, 101 (2010)
19. M. Comotti, C. Della Pina, R. Matarrese, M. Rossi, Angew. Chem. Int. Ed. **43**, 5812 (2004)
20. H. Okatsu, N. Kinoshita, T. Akita, T. Ishida, M. Haruta, Appl. Catal. A Gen. **369**, 8 (2009)
21. F. Porta, M. Rossi, J. Mol. Catal. A Chem. **204**, 553 (2003)
22. M.R. Ali, Y. Wu, S. Chapman, Y. Ding, Res. Chem. Intermed. **45**, 3973 (2019)
23. Y.C. Zhao, D.L. Yu, H.W. Zhou, Y.J. Tian, O. Yanagisawa, J. Mater. Sci. **40**, 2645 (2005)
24. R. Zanella, S. Giorgio, C.R. Henry, C. Louis, J. Phys. Chem. B **106**, 7634 (2002)
25. E.V. Murzina, A.V. Tokarev, K. Kordás, H. Karhu, J.P. Mikkola, D.Y. Murzin, Catal. Today **131**, 385 (2008)
26. E. Smolentseva, B.T. Kusema, S. Beloshapkin, M. Estrada, E. Vargas, D.Y. Murzin, A. Simakov, Appl. Catal. A Gen. **392**, 69 (2011)
27. S. Brunauer, P.H. Emmett, E. Teller, J. Am. Chem. Soc. **60**, 309 (1938)
28. E.P. Barrett, L.G. Joyner, P.P. Halenda, J. Am. Chem. Soc. **73**, 373 (1951)
29. B.C. Lippens, J.H. de Boer, J. Catal. **4**, 319 (1965)
30. R. Wojcieszak, I.M. Cuccovia, M.A. Silva, L.M. Rossi, J. Mol. Catal. A Chem. **422**, 35 (2016)
31. P.N. Amaniampong, A. Karam, Q.T. Trinh, K. Xu, H. Hirao, F. Jérôme, G. Chatel, Sci. Rep. **7**, 40650 (2017)
32. M. Zhou, F. Pu, Z. Wang, S. Guan, Carbon **68**, 185 (2014)
33. S.N. Talapaneni, S. Anandan, G.P. Mane, C. Anand, D.S. Dhawale, S. Varghese, A. Mano, T. Mori, A. Vinu, J. Mater. Chem. **22**, 9831 (2012)
34. X.B. Hu, Y.T. Wu, H.R. Li, Z.B. Zhang, J. Phys. Chem. C **114**, 9603 (2010)
35. J. Wang, R. Huang, Y. Zhang, J. Diao, J. Zhang, H. Liu, D. Su, Carbon **111**, 519 (2017)